Localized skin Disease Detection and Classification using an optimized Hybrid Deep Learning Model with Attention Mechanism

Dr. Ranju S Kartha

Assistant Professor, Department of Information Technology, Rajagiri School of Engineering and Technology, Cochin

Abstract

Deep learning systems are good identifying the traits obligatory to precisely comprehend multifaceted sequences. This work put up a deep learning-based attention GRU for a computerised method of identifying skin diseases. The portable computing device-compatible attention GRU paradigm has been demonstrated to be accurate and reliable. For accurate projections, the recommended approach effectively preserves stateful data. The system's efficiency has compared various cutting-edge models, including Fine-Tuned Neural Networks (FTNN), Convolutional Neural Networks (CNN), and Highly Deep Convolutional Networks for Large-Scale Image Identification developed by the Visual Geometry Group (VGG). On the HAM10000 dataset, the proposed strategy performs better than cutting-edge techniques with over 85% efficiency. It requires less processing effort because of its resilience in recognising sooner and with more severity than the affected area nearly two times fewer calculations than the traditional attention GRU approach. It helps individuals and dermatology identify the type illness using an image of the affected area in the early stages of skin sickness. These findings show that the recommended strategy can help medical practitioners identify skin abnormalities quickly and precisely, hence averting morbidity and future issues.

Keywords: Convolutional Neural Networks, Fine-Tuned Neural Networks, Hybrid Deep Learning, Gated recurrent unit.

1. Introduction

Billions of people throughout the entire globe are affected by skin conditions, which are among the primary drivers of disease burden. Having approximately 3000 entities documented in the scientific literature, ageing, environmental and genetic variables, trauma, and other factors can all provide something to the development of a wide range of skin sicknesses [1]. In order to give mechanical or immunologic security in a not sterile land surroundings, human skin goes through major modifications as it moves from an aquatic environment that was largely pathogen-free in gestation [2]. Persistent inflamed skin conditions damage an individual's happiness with life in terms of their physical, material, social, and psychological well-being [3]. Each day, it has an impact on hundreds of millions of individuals. Skin infection and skin neoplasm, among the hundreds of skin disorders, are the two main types of skin illness [4]. The three primary triggering events that cause skin changes while pregnant are as follows: three factors: (i) a rise in circulating hormone levels; (ii) an increase in intravascular volume; and (iii) compression due to the growing uterus [5]. The serious condition lumpy skin disease (LSD), which affects calves and water buffalo, is considered by many cutaneous lumps. It brought on by infection with Capri pox virus genus' poxvirus lumpy skin disease virus (LSDV). Hematophagous vectors that disseminate the LSDV virus quickly under favourable environmental circumstances include mosquito and insects [6] [7].

Data-driven assessment is essential because skin disorders tend take a variety of shapes, inadequate numbers of trained dermatology specialists, and they're dispersed incorrectly. Deep learning models execute the method of categorization from the data and images rather effectively [8] [9] [10]. DL algorithms are reaching human-level effectiveness in several domains thanks to both the Internet's huge availability of information and increase processing power offered by cutting-edge technology. CNNs, for instance, contributed to significant advancements in area of therapeutic imaging processing, especially for MRI, CT, and pathology imagery, which contain stiff features with excellent resolution [11]. A simple in-vivo imaging method called dermoscopy, especially or epiluminescence microscopy reveals specific morphological and visual characteristics of coloured lesions [12]. Skin cancer that is lethal in its early stages and sometimes mistaken as a benign skin lesion is melanoma. In the United States, melanoma is thought to cause 76,380 new cases and 6,750 fatalities annually [13].

The healthcare sector takes considerably benefited from abundance medical data produced by cutting-edge physiological signal and imaging technology, but the expense of data processing has also significantly grown. In order to emulate human specialists, AI technology adept summarising decorations in massive volumes of records. As a result, AI-enhanced healthcare systems are crucial to every aspect of the healing process, including precise diagnosis, rehabilitation, and preventative medicine [14]. Convolutional neural network (CNN)-based methods have greatly outperformed conventional methods in that they can directly learn important characteristics from data [15] [16] [17].

Contribution

- The researchers proposed a novel model that combines the power of deep learning and attention mechanisms with the GRU architecture.
- The attention GRU model designed to run on portable computing devices, making it accessible and practical for use in various settings.
- Stateful data are effectively preserved by the proposed paradigm, allowing for precise forecasts.
- The attention GRU model shows resiliency by identifying the affected area much more quickly and with fewer calculations compared to the traditional attention GRU approach.
- The proposed method proves valuable in early stages of skin illness by aiding doctors and patients can identify the condition from a picture of the affected area.

The contented of this paper is organized in the ensuing manner: Section 2 examines earlier research on skin disease using various optimization methodologies. Section 3 describe problem statement, section 4 briefly explained proposed method pre-processing, feature selection and classification. Section 5 is result and discussion, section 6 experiment article is concluded with section 7 and evaluation.

Related work:

An, Li, and Ma. [18] proposed incorporating an optical attention system into the deep learning framework allows for more precise thinking and more efficient extraction of data in response to the challenge of medical images. It could make the model easier to comprehend. Furthermore, paper resolve create a novel multistate CNN model that is capable of extracting elevated prejudiced characteristics of the original image's look in order solve problem corresponding deep learning network's framework training method to medical images. To acquire an improved retraining methodology and enhance the connection mode's resilient achievement, the loss function technique additionally applies a Mahalanobis distance optimisation model. The classification of medical photos is completed by the aforementioned method. In considering the previously discussed concepts, this study offers a therapeutic categorization method based on a visual attention mechanism-multiscale CNN. The approach described in this research was used to categorise photos of breast cancer and lung nodules. The results of this research indicate that the strategy is stable and resilient, and that the accuracy of medical picture categorization in this study is superior to alternative deep learning approaches as well as regular process for machine learning.

Fu et al.[19] proposed in order to classify and localise MI with 12-lead ECG data, a novel multi-lead attention (MLA) mechanism linked with CNN and bidirectional gated recurrent unit (BiGRU) structure is suggested (MLA-CNN-BiGRU). In particular, the MLA system automatically determines and weighs the various leads in accordance with their contributions. The two-dimensional CNN component extracts discriminative spatial features by taking use of the relationships between leads' traits. Additionally, each lead's critical temporal properties are extracted via the BiGRU module. The time and space data in both of these components is combined to produce international traits for grouping. To evaluate robustness of the proposed framework, MI translation and recognition were conducted in trials interpatient as well as intrapatient scheduling arrangements. According to findings from experiments, the smart framework carried out adequately and revealed significant medical value.

Wu et al. [20] proposed ADAM has the capacity to gather more detailed and distinct information for identifying the border of skin lesions. In order to even more increase segmentation accuracy, the suggested ADAM allows multi-scale resolve fusion and may therefore collect multi-scale characteristics. Third, compared to conventional CNNs, our technique may significantly minimise redundancy since it makes use of a spatial information weighting mechanism in the proposed network. The dual encoder design used in the suggested network allows for an expansion of the responsive field without significantly raising the network's parameters. Additionally, we give several ADAMs various dilation rates so that it can adaptably record distinctive characteristics in accordance with the extent of a lesion. Everyone thoroughly test the suggested approach on the ISBI2017 and ISIC2018

information sets, and our experiments show that, without the use of network ensemble schemes, our method is capable of outperforming contemporary deep learning algorithms, especially those with mechanisms for focus, in terms of the accuracy of segmentation.

Pramanik et al.[21] proposed a procedure that has two primary steps for classifying breast mass using mammography. Initial include a system for attention into the well-known VGG16 model to abstract deep features from the input mammograms. To get an ideal features subset, we then employ a meta-heuristic dubbed the Social SkiDriver (SSD) method, which is integrated with Adapted Beta Hill Climbing based local search. The k-near neighbours (KNN) classifier does the classification using the best data subset. It is shown that the suggested model is quite helpful for correctly detecting and discriminating healthy and cancerous breasts. Using digital database for screening mammography (DDSM) database as a testing ground, we analyse our model and obtain 96.07% accuracy with just 25% of the information collected through the attention-aided VGG16 model.

Alzahrani, Al-Bander et al. [22] proposed automatic severity of acne rating and counting approach using face photos. To achieve this, they create a multi-scale inflated completely convolutional regressor linked into an attention mechanism for dense map construction. With dilated convolution filters, the proposed fully convolutional regressor module modifies UNet to methodically collect multiscale contextual data for density map construction. They add an attention mechanism to the regressor model that is represented by previous limit box knowledge produced by Faster R-CNN. By identifying some of the most prominent traits associated with the neglected acne lesions, this focus mechanism directs the regression models on where to seek the actual acne lesions, enhancing its resilience to various face acne lesion distribution in thin and dense areas. Number of acne lesions image is obtained through the integration over the density maps that have been created, and the number of lesions corresponds to the intensity of the acne. The obtained findings show enhanced performance regarding regression and organisation metrics when compared to current methods. The created using a computer-based diagnostic instrument substantially aid and assist automatic grading of the severity of acne lesion, greatly lowering the effort associated with human evaluation and assessment.

The apparent resemblance of the healthy and affected skin region, as well as artifacts such gel bubbles, hair, and clinical markings, however, point to low accuracy rates. Albahli et al. [23] developed a method to overcome this difficulty .In the first step, image regions are sharpened and artifacts gel bubbles, marks hairs are eliminated from the dermoscopic pictures using morphological processes and retrieved using the active contour segmentation strategy . ISIC2018 and ISIC2016 datasets were used. Accuracy is 94%. which Can be improved by effective segmentation method. Application of the skin enhancement phase results in a little loss of image information,

Yao et al.[24] suggested an innovative single-model based approach categorization of skin lesions on unbalanced data. In order to demonstrate that algorithms with moderate difficulty outperform the more complicated models, a variety of DCNNs are first practised on several different small and asymmetrical datasets. Second, combat flaws of sample under representation in the short dataset, regularization DropOut and DropBlock are introduced to a modified RandAugment, which decreases overfitting enhancement approach is suggested. In low resource contexts, it might be implemented mobile strategies for automated detection of Because it achieved a strong classification accuracy at a low cost of computing resources and inference time, it was used to diagnose skin lesions and many different cancers. Since the size of feature maps in these models require vast amounts of memory.

2. Problem statement

Due to the broad variation color, look, shape, then the presence artefacts like hair, gel bubbles, clinical rule marks, it is difficult to identify skin lesions precisely from dermoscopic pictures. Hence, skin refinement steps were developed. In which skin enhancement process is used to reduce artefact occlusions and enhance the segmentation of melanoma lesions[23]. But, application of the skin enhancement phase results in a little loss of image information. Reduction of overfitting is another difficult task. First, Dropout and Drop Block are combined to create a new DCNN model. Second, a modified Rand Augment approach is suggested that is more suited for the data from the dermoscopic images. Because of that the size of the feature maps in these models require vast amounts of memory [24].

3. Proposed method

Gather a dataset of skin disease images with corresponding labels. In this case, the HAM10000 dataset has been used for evaluation. Preprocess dataset by consistently resizing the photographs resolution, dividing it into test and training sets, and normalising the pixel values. Design the deep learning-based attention GRU model

architecture. It typically consists of layers such as convolutional layers for feature extraction, recurrent layers (such as GRU) for sequential modeling, and attention mechanisms for focusing on relevant regions. Train the attention GRU model using the training set. During training, optimize the model parameters using techniques like backpropagation and gradient descent, minimizing a suitable loss function. Figure 1shows flow diagram of skin disease categorization and detection utilising an optimized hybrid deep learning model.

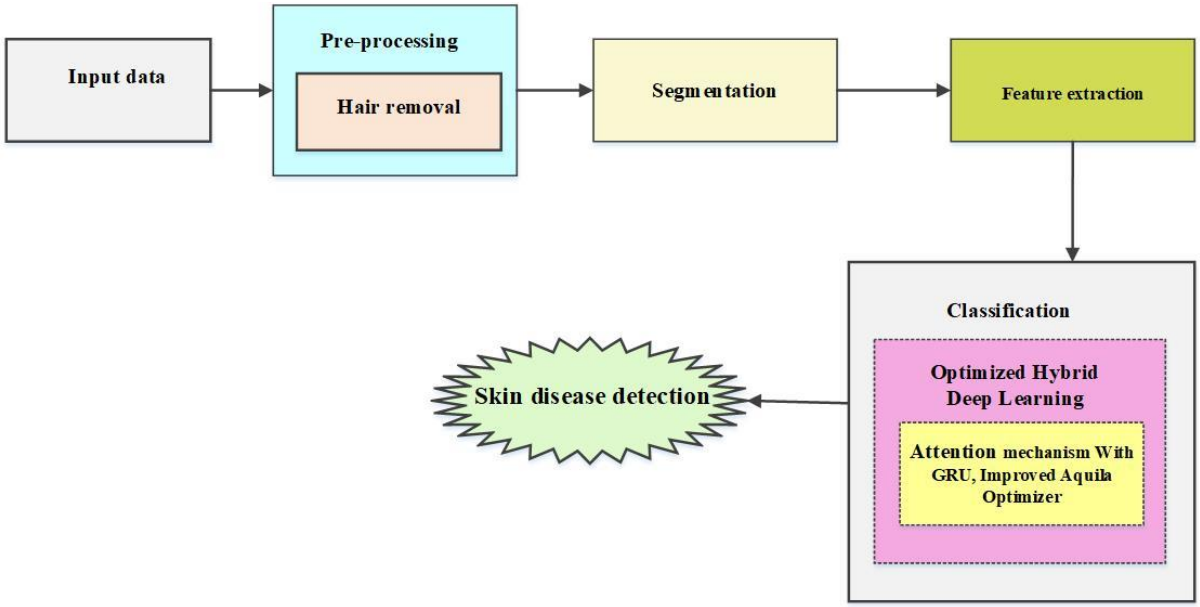

Figure 1: flow drawing of skin disease detection and classification using an optimized hybrid deep learning model

4.1. Data collection

The dataset is essential to development of neural networks we suggest using for automatic diagnosis. The skin disease dataset, designated HAM10000, was taken from Kaggle, which was used as an example database retrieved from the original source. The dataset includes gender, age, and type of cell in the form of metadata in a values separated by comma file (.CSV). More than 10,000 dermatoscopic imagery from various people throughout the world are included in this collection. The information set also offers further advice on how to deal with issues like overfitting and data scarcity, which will assist improve the model's efficacy and accuracy. The amount of skin photos for each type of lesion in the sample is unbalanced. Techniques for augmenting data were utilised to balance all sorts of grazes to same range pictures in order to prevent this disparity. To improve the generalizability of our model, the dataset is split into three sections: training data, testing data, and validation data, each including 85%, 5%, and 10% of the total data. The training dataset's accompanying real-world data is used to test the model. For our suggested model, an image's goal size is 224 by 224. This study seeks to evaluate the precision of our suggested method for skin cancer diagnosis using dermatoscopic visuals [25].

4.2. Pre-processing

Pre-processing is the initial and most important stage in consider analysis. The two potential enhancing approaches mentioned in the suggested strategy are the median filter and histogram equalisation. The median filter selects the input imagery, arranges the pixels in the order of ascending, selects its centre value, and then swaps out the old value with the newly created value. The histogram equalisation improvement approach now receives the result of the median filter as an input. Both operations are carried out in the domain of space. The median filter's output is organised on different pixel levels. The running sum is computed, divided by the running sum's total number, and then each element is multiplied by the sum of the grey level values to produce the final result.

4.2.1. Hair removal

An image that has been histogrammed is given into the pre-processing stage of the hair eradication procedure. Hair removal is done on human skin since hairs are present on every part of the body, regardless of the input. The removal of hair may be accomplished by applying morphology operator to the input picture, applying the bottom hat transform, finding the long and thin objects, and then obtaining the final output utilising marker ideas [26].

4.3. Segmentation

The segmenting phase comes after the preliminary processing step and is carried out here because segmentation aids in identifying the region of requirement. Compares the background and foreground images using the determined histogram, and we take into account computations for up to seven intensity levels and seven total values using the formula following.

$$\sigma_c^2 = C_z\sigma_z^2 + C_V\sigma_V^2 \quad (1)$$

With the use of this technique, that can identify the pixels that make up an image's backdrop and other and compare the number of pixels we locate to the total number of background and foreground pixels. Next, the associated foreground and background's average and variation are estimated. The background brightness multiplied by the variance of the backgroundσ_z^2, as well as the weight of the background imageC_z, are explained by Eq. (1).The background weight is then calculated, and the associated level is increased by the foreground variationσ_V^2. The totaling value is created by adding these two. The value is then determined using the weight, the variance, and several thresholding values.

4.4. Feature extraction

The third crucial stage in the detecting process is feature extraction. The comparable characteristics in our research, which must be chosen. The common method and the area may be used to compute the mean, variance, and standard deviation. When it comes to categorization, features are crucial, and feature extraction also aids in detection. The different qualities that are taken into account while determining how to extract features. In this section they provide our methodology's area, mean (mea), variance (Var), and standard deviation (SD), all of which may be determined using conventional methods. They employ the fundamental statistics approach, yet there are other feature extraction methodologies as well, such as the Gabor filters. In the future, we'll strive to add additional characteristics to further increase classification accuracy. The accuracy of the categorization depends greatly upon the extracted characteristics. The process of extracting features and feeding them to classifiers is described in the table below. The table describes numerous characteristics that are taken into account, including area, variance, standard deviation, and mean. Furthermore, the mean is determined using the accepted formulas; it is the sum of all values divided by the total number of components. Similar calculations are used for variance, standard deviation, and area. The properties mentioned above can be checked to do a texture analysis since they are supplied as input to the classifiers. The study that is done enables us to compare the results of all the employed classifiers and determine which one has the best classification rate.

4.5. Attention mechanism Classification using an optimized Hybrid Deep Learning

The attention mechanism arose from the fact that while identifying anything, the human part would give greater attention to only particular portions. It becomes one of most extensively used techniques in natural language processing. Few studies integrate attention mechanism with GRU network and utilize it anticipate economic series regularly influenced several difficult factors at same time. In the input series are equally essential to anticipated value at each time t when forecasting energy price series. Primary idea behind the attention mechanism is pay further attention to relevant information in order to perform more neuronal processes, rather than taking all elements into consideration equally. The three implementing phases for calculating attention value are shown in figure, whereby the system can start giving different weight to an element in the input sequence at different periods. Figure 2 shows attention value calculation. The procedure may state as follows [27]:

Step 1: Determine the importance of $J_{tr,}r = 1,2,...,r$ each previous data element and output element at a given time point$t$, as indicated by the attention score $e_{tr} = Attend(x_{tr})$.

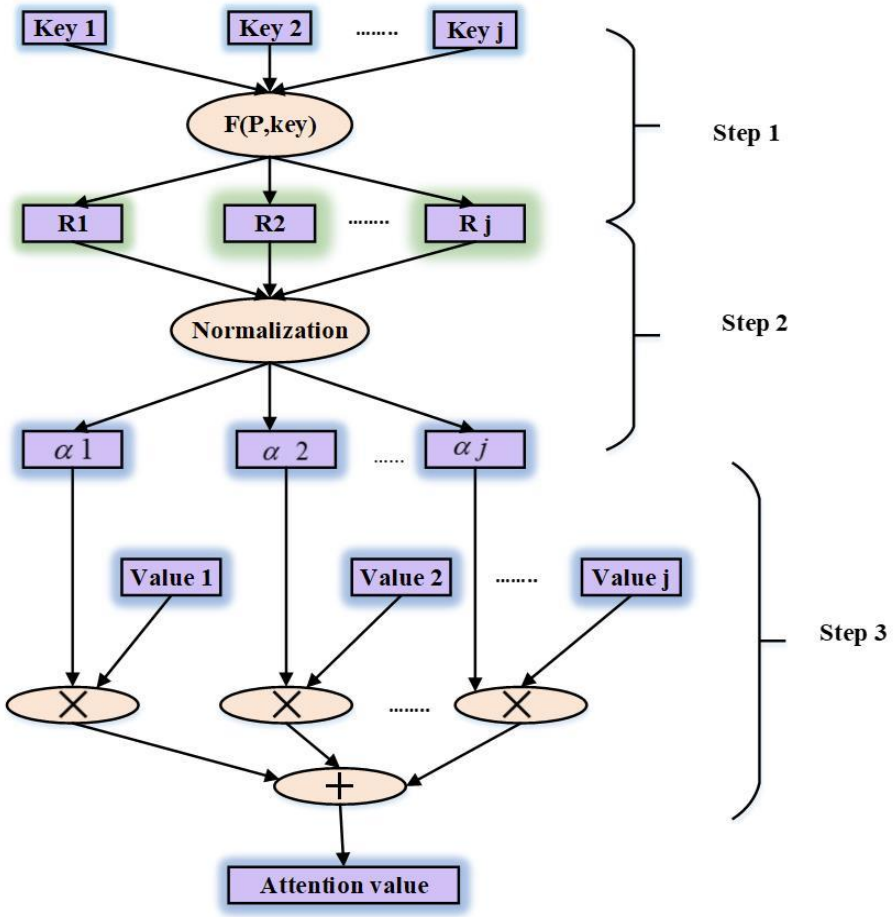

Figure 2: Attention value calculation.

Step 2: Softmax function converts the relevancies into probability, attention weight of the r^{th} element of the input sequence at time t indicated by α_{tr}.

$$\alpha_{tr} = \frac{\exp(e_{tr})}{\sum_{r=1}^{r} \exp(e_{tr})} \tag{2}$$

Step 3: To indicate the components' contribution to the anticipated value, multiply the probability obtain in step 2 by the implied symbol of the relevant input elements. Then, as input components, add up the contributions of all input parts to forecast the following value. The original input x_t replaced by biased feature $\tilde{x}_t$, which used, as neural network input and written as:

$$\tilde{x}_{tr} = \alpha_{tr} x_{tr} \tag{3}$$

4.5.1. Gated recurrent unit (GRU)

The GRU network reconstruct the LSTM cell's gating mechanism while retaining its quality. Every GRU cell has two gates: the reset gate j_t and update gate b_t. The reset gate, like LSTM, governs how much old information is kept and how much new information is supplied at this time, assisting in the capturing of periodic correlations in data. The update gate controls degree which past knowledge is "forgotten," and data of unlimited length of input x_t may effectively memorised inside the gate. The number of parameter in the GRU cell is substantially lower than the LSTM, as shown in figure 3, demonstrating that the GRU structure is simpler than

the LSTM structure. Because of GRU network is variant of LSTM network, it can utilised to solve issue of long dependences ordinary RNN networks.

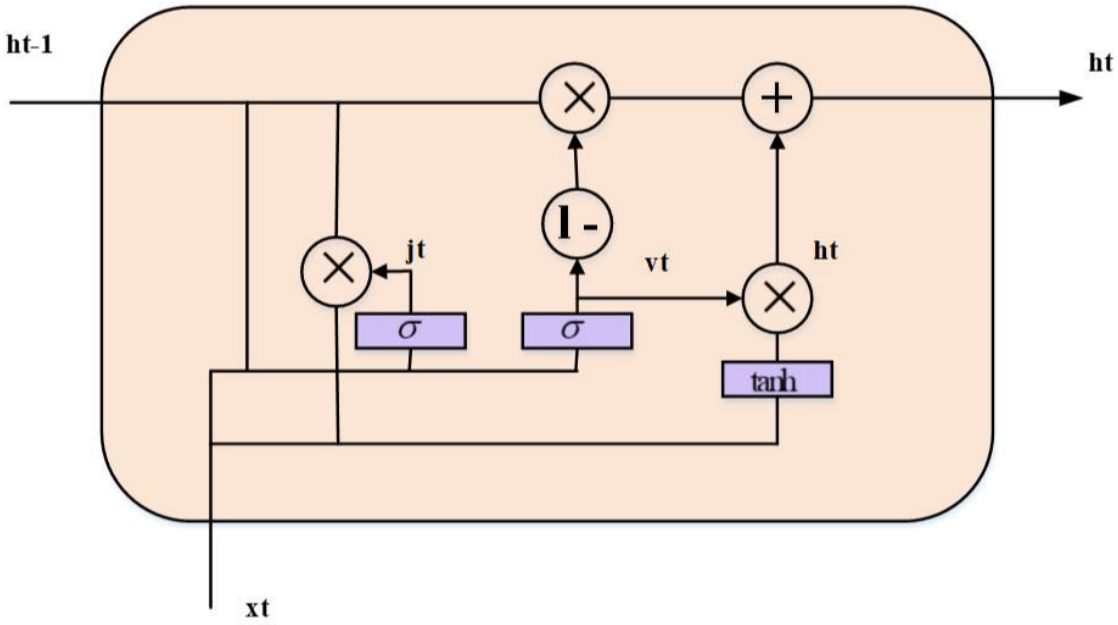

Figure 3: Structure of GRU

GRU's fundamental steps are as follows:

First, the latest input x_t is the hidden condition established by the previous cell h_{t-1} reset gate j_t then apprise gate v_t at recent state (time t). The two gates' output is as follows:

$$j_t = \sigma(w^j[h_{t-1}, x_t] + b^j) \tag{4}$$

$$v_t = \sigma(w^v[h_{t-1}, x_t] + b^z \tag{5}$$

Where w^j and w^v are the proper matrix of weight coefficients, b^j and b^z are bias vectors, and $\sigma()$ is sigmoid function.

Next, nearby applicant concealed municipal $\tilde{h}_t$ expressed as monitors:

$$\tilde{h}_t = \tanh(w^h[(h_{t-1} * j_t), x_t] + b^h) \tag{6}$$

Where $\tanh$ tangent hyperbolic operation, w^h are relevant matrix weight coefficients for the buried layer, b^h is associated bias vector, and * denote matrix of dot development between pairs.

Finally, consider the present hidden state h_t output is determined linearly combining current candidate hidden state $\bar{h}_t$ and before-hidden state h_{t-1}, with total with adjusted coefficients of 1:

$$h_t = (1 - v_t) * \bar{h}_t + v_t * h_{t-1} \tag{7}$$

Machine learning methods are dynamic since they often contain multiple parameters that must be turned for maximum performance, and manually optimising data may be exhausting as well as stressful. In this work, is to improve the performance of ATTGRU by selecting optimal weight parameters. The input layer, two

levels of AttGRU hidden layer, complete connection layer, and output layer comprise the structure of the GRU model projected this study. The HMWSO method is throughout model training phase to optimise the weight and bias in the AttGRU network. The time step, batch size, and number of hidden layer units are configured as GRU model hyper parameters in this model.

To utilize the dataset's training portion to compute each configuration's quality using the fitness function shown below. (i.e., it is the root mean square error):

$$fit = MSE = \frac{1}{N_y}\sum_{q=1}^{N_g}(T_q - P_q)^2 \tag{8}$$

where, T and P denotes the actual and predicted output, the sum of training samples is denoted by N_y.

4.5.2. Improved Aquila Optimizer (IAO)

Aquila's natural hunting behaviour inspired this approach. Based on the benchmarking capabilities of the statistical results, the admirably performed AO algorithm finds the best solution. However, in other traditional optimization procedures, exploration and exploitation capabilities of AO algorithm can still be improved. The primary idea behind enhanced algorithms is to improve accuracy and keep balance between global search and local mistreatment capabilities used to avoid untimely convergence and increase convergence speed. Consequently, the original AO algorithm was enhanced with two improvement procedures [28].

Random initialization is used to produce the initial population of weight X. The formal appearance as follows:

$$X_{qr} = LB_r + rand \times (UB_r - LB_r),\ q = 1,2,....,P, r = 1,2,.....,D \tag{9}$$

here, X indicates set of current x solutions randomly created $rand$ is random number between 0 and1, P indicates population size, and D denotes the problem dimension. The maximum and minimum values for the search agent in r^{th} dimension search space are represented by UB_r and LB_r, respectively.

Here, X identifies and selects the optimal location X by conducting a soaring high stooping vertically (X_1). The AO investigates the search sector for the best location X from a great height.

$$X_1(t+1) = X_{best}(t) \times (1 - \frac{t}{T}) + (X_M(t) - X_{best}(t) \times rand) \tag{10}$$

Here, $X_1(t+1)$ is next iteration's solution t created. $X_{best}(t)$ is most useful key found until t^{th} iteration, it depicts approximate position optimal X. $(1 - \frac{t}{T})$ is employed to limit number of iterations in the extended investigation. $X_M(t)$ is mean of all available options during t^{th} iteration. $rand$ is a number between 0 and 1. The amount of iterations in progress is t, and the most iterations allowed is T.

$$X_M(t) = \frac{1}{P}\sum_{q=1}^{P} X_q(t),\ \forall r = 1,2,....,D \tag{11}$$

Where, D problem measurement and P is population number.

Here, the optimal X is discovered using Aquila's contour flying method with a short glide. The Aquila circles over intended prey to catch its prey; likewise, the optimal X can also be detected and is mathematically expressed as,

$$X_2(t+1) = X_{best}(t) \times levy(D_s) + X_{Ra}(t) + (y - x) \times rand \tag{12}$$

here, $X_2(t+1)$ indicates the following iteration t created, i.e. X_2, D_S denotes the dimensional space, $levy(D_s)$ represents the levy for the flight distribution function. In t^{th} iteration, $X_{Ra}(t)$ is random solution picked from N solution.

$$levy(D_s) = c \times \frac{u \times \sigma}{|\upsilon|^{\frac{1}{\beta}}} \tag{13}$$

here c is anupdated constant of 0.01, u and υ are random values between 0 and 1.

The following formula is used to calculate σ value:

$$\sigma = \left(\frac{\gamma(1+\beta) \times \sin(\frac{\pi\beta}{2}}{\gamma\left(\frac{1+\beta}{2}\right) \times \beta \times 2^{\frac{\beta-1}{2}}} \right) \tag{14}$$

Here β is a fixed constant value 1.5.The spiral from process is represented y and x, and the equation:

$$y = r \times \cos(\theta), x = r \times \sin(\theta) \tag{15}$$

$$r = r_1 + F \times I_1 \tag{16}$$

$$\theta = -\omega \times I_1 + \theta_1 \tag{17}$$

$$\theta_1 = \frac{3 \times \pi}{2} \tag{18}$$

Where, r_1 set the count of search cycles, enter a value between 1 and 20, and F is a constant of0.00565. I_1 positive numeral between 1 and length of search space (I), and ω is a permanent value of 0.005.

Here, X is accurately identified by using the technique of low flying of Aquila with a slow descent attack (X_3). Aquila is prepared land and begins its descent with a preliminary attack vertically to identify its target. Likewise, the optimal X can also be detected and is mathematically expressed as,

$$X_3(t+1) = (X_{best}(t) - X_M(t)) \times \alpha - rand + ((UB - LB) \times rand + LB) \times \delta \tag{19}$$

here, $X_3(t+1)$ are results of third search way's following iteration of t, $X_{best}(t)$ represents approximate location of optimal X after the i^{th} iteration (optimal value) and $X_M(t)$ shows the present solution's cruel value the t^{th} iteration. $rand$ is a number chosen at randomly between 0 and 1. α and δ are exploitation adjustment variables have been set at 0.1. UB and LB problem's upper and lower limits, respectively

Here, X is identified based on its stochastic motions using the fourth technique (X_4),walk around and catch prey. The Aquila goes for a walk and grabs its prey; likewise, the optimal can also be detected and is mathematically expressed as,

$$X_4(t+1) = QuF \times X_{best}(t) - (V_1 \times X(t) \times rand) - V_2 \times loss(D) + rand \times V_1 \tag{20}$$

Where, $X_4(t+1)$ represents explanation obtained by next iteration of t is generated by (X_4). QuF is optimize the search technique, the quality function is applied, and it is determined using Eqn.(21). V_1 isthe Aquila tracking prey's varied motions, created using equation (22). V_2 indicates thatequation (30) produces a decreasing number from 2 to 0.The currently available solution in the t^{th} iteration is $X(t)$.

$$QuF(t) = t^{\frac{2 \times rand - 1}{(1-T)^2}} \tag{21}$$

$$V_1 = 2 \times rand - 1 \tag{22}$$

$$V_2 = 2 \times \left(1 - \frac{t}{T}\right) \tag{23}$$

Here, $QuF(t)$ is superiority function's value in t^{th} iteration besides $rand$ is a random number between 0 and 1.

5. Result and discussion

The experimental setup, performance measurement, evaluation datasets, and experimental outcomes are all described in this section. The findings discussion includes an assessment of the suggested attention mechanism GRU- IAO work scheduling techniques. The model performs well on the test data, which an important indicator of its efficiency is given that the model has never seen the data before. The suggested strategy for predicting skin disease and assessing the outcomes, the cardiovascular dataset was pre-processed at the start with segmentation. To increase the model's impact and stability tested a variety of network optimization approaches.

5.1. Simulation environment

Tested the suggested Attention GRU- IOS technique using python software in a simulated environment utilizing cardiovascular dataset. The test are run on a machine equipped with an Intel(R) Core i5-3630 CPU @ 3.20GHz, 3200 Mhz, 3 core(s), 3 logical pro. And the micro software 10 pro, micro soft corporation is an OS manufacturer, installed physical memory (RAM) 8GM.

6. Experimental evaluation

The authors made the decision to standardise crucial parameters across all experiments in order to make a fair comparison between alternative techniques regarding their execution settings. How well the suggested approach performs in practise is determined by statistical analysis using a variety of effectiveness evolution criteria, including but not limited to accuracy measurements. The suggested framework successfully categorises the skin disease often. The study was initially run on a number of photos, and the type of disease is determined using the suggested method.

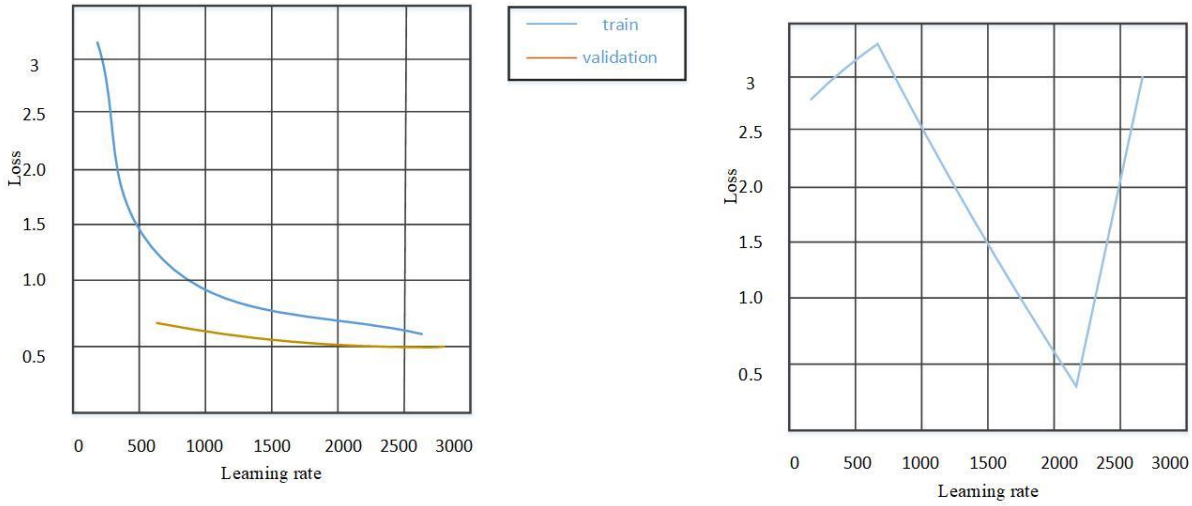

Figure 4: Resultant consequences post optimizing training rate.

Graphs in Figure 4 were created using the model training loss from the initial trained model was lower verification model loss. Left graph shows how many sets were handled in relation to the loss discovered during training and validation phases. The first model uses a batch size value of 100 to expedite the training data. The rate at which learning occurs is shown together with both training and validation loss.

Table 1: performance metrics for various methods

Algorithms	Sensitivity	Specificity	Accuracy	JSI	MCC
HARIS [29]	78.3	83.01	77	83.01	77
FTNN [30]	79.54	84	79	84	79
CNN [31]	80.41	85	80	85.16	80
VGG19 [32]	82.46	87	81	86.71	81
MobileNet V1 [33]	84.04	89	82	88.21	83

MobileNet V2 [34]	86.41	90	84	89.95	84
Proposed	95.1	96.3	97.3	98.5	96.2

In Table 1 compares the performance of our suggested technique with that of other relevant approaches. The suggested model had the highest efficiency in identifying diseases, whereas the proposed models performed better in categorising the region of interest with the least amount of computational effort.

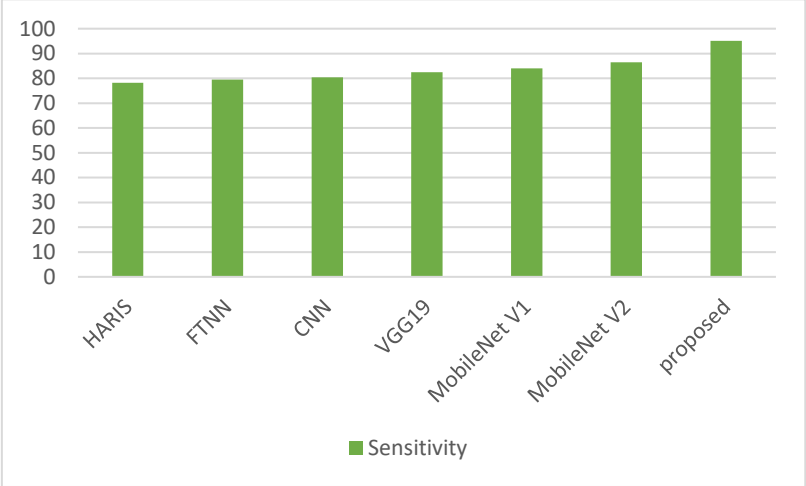

(a) Sensitivity graph compared various methods

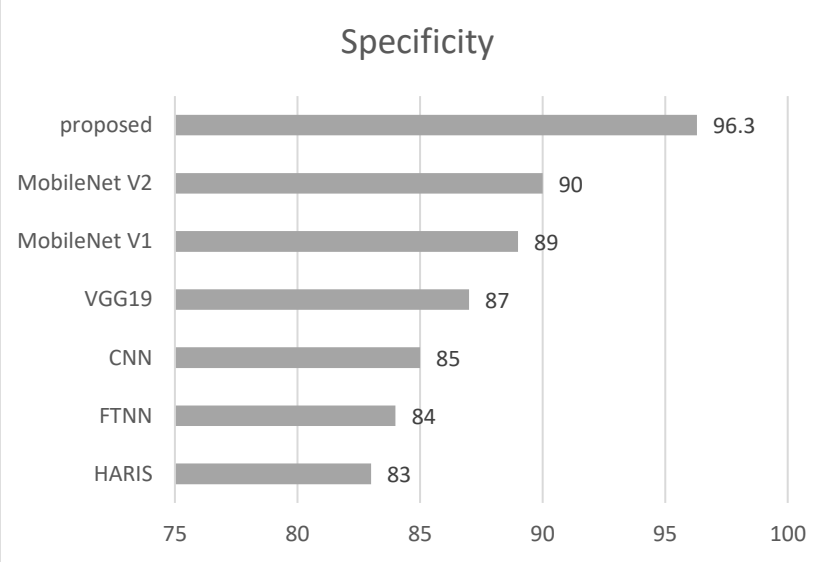

(b) specificity graph compared various methods

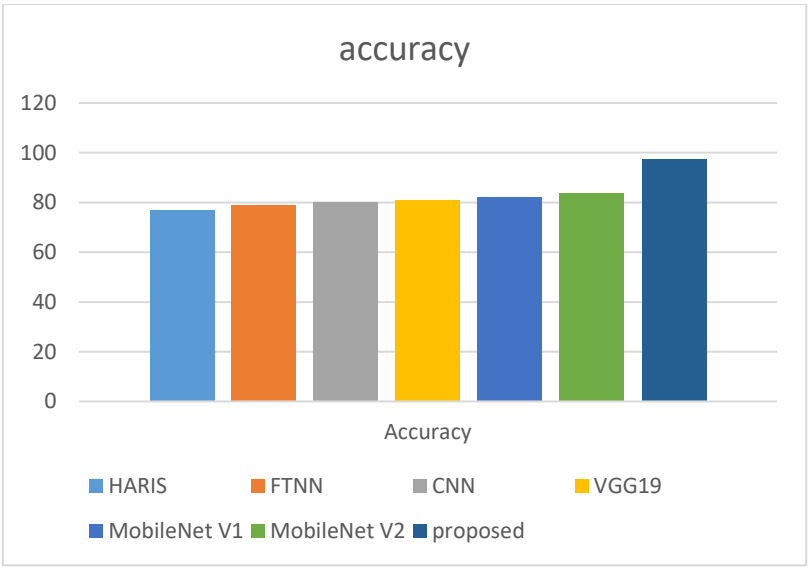

(c) accuracy graph compared various methods

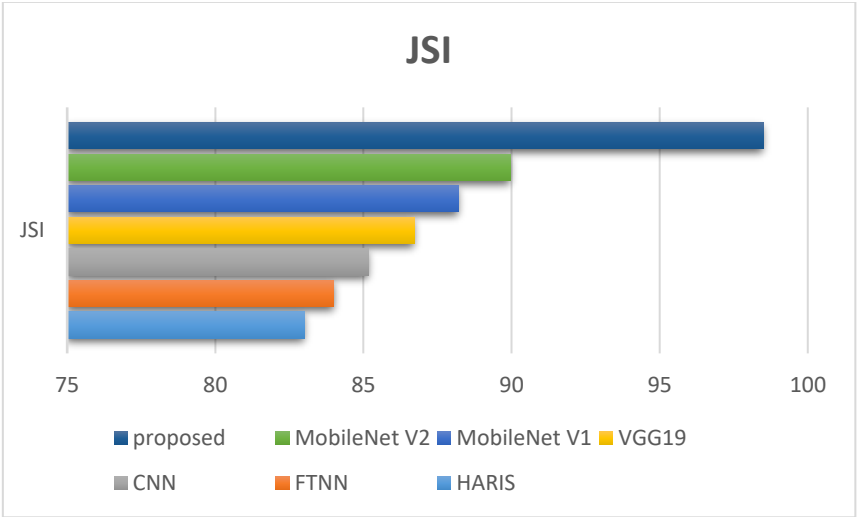

(d) JSI graph compared various methods

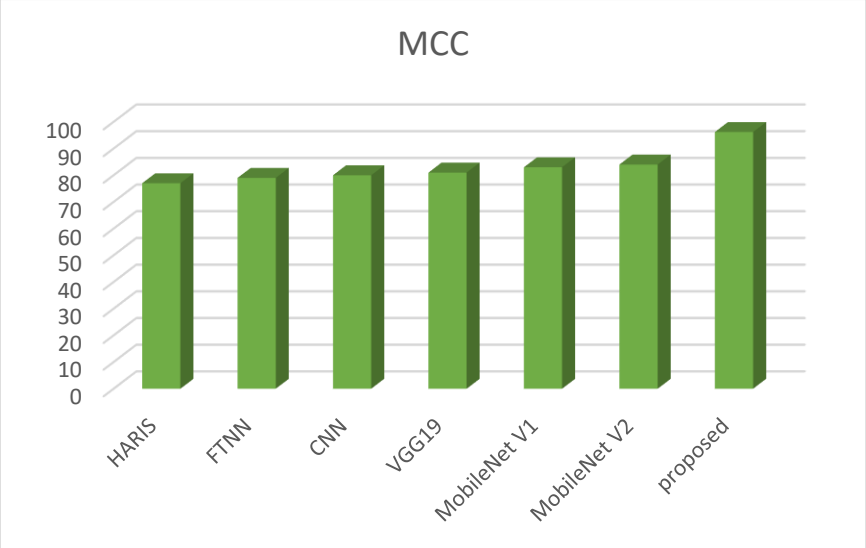

(e) MCC graph compared various methods

Figure 5: comparison metrics with various methods (a) Sensitivity (b) specificity (c) accuracy (d) JSI (e) MCC

The testing procedure is repeatedly run on the auxiliary computer on multiple executions of the simulation in order to assess the effectiveness. The assessments are based on how frequently the suggested model properly categorises skin illness that deemed True Positive and correctly recognises image is not specific skin category True Negative. Number of times suggested model accurately identifies condition referred to as the False Positive rate. Expected False Negative is the number of times suggested model analyses the skin illness incorrectly. Figure 5 assessing the suggested model's sensitivity, specificity, and accuracy, metrics such as True Positive, True Negative, False Positive, and False Negative are taken into account.

Table 2. The progress of the disease growth.

Algorithms	**Disease of Core (DC)**	**Whole Disease of Area (WD)**	**Enhanced the DISEASE (ED)**	**(Mean Value)**
HARIS	8.854	12.475	3.621	0.92
CNN	8.894	12.498	3.604	0.89
FTNN	8.903	12.522	3.619	0.91
proposed	9.6	13.4	5	0.95

The result of calculating the average of the confidence values seen during repeated experiments is shown in Table 2. The mean of the evaluated confidence value can be used to gauge how resilient the suggested technique is. The figures after the decimal point show how far the estimates are from the actual data. In comparison to the other approaches reviewed in the research, the values for the suggested methodology are almost insignificant.

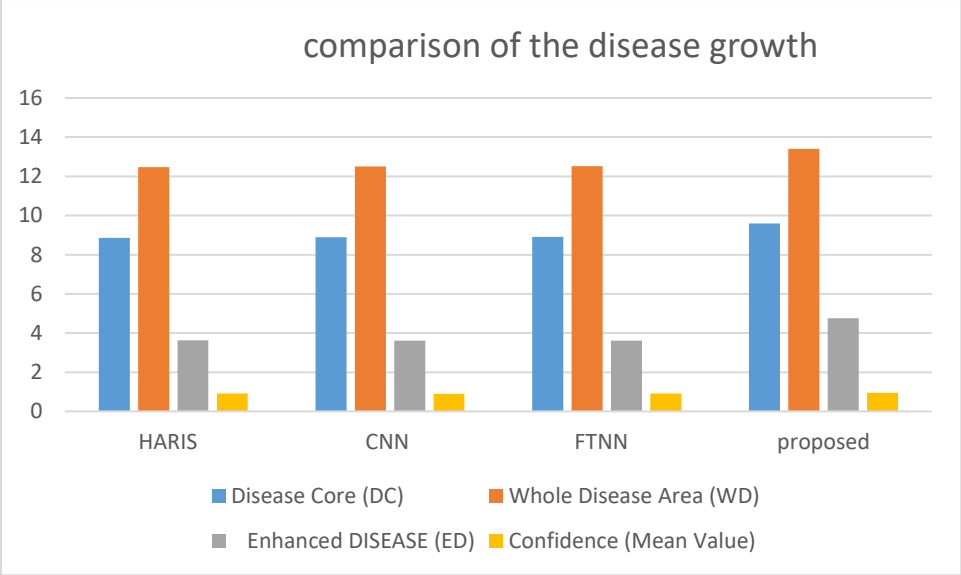

Figure 6: comparison graph for disease growth

Figure 6 showing progression of disease might help patients receive better care. The model is effective in determining how sick growth is developing. The sureness value establishes average degree of confidence at which the disease's increased part is identified. The suggested model effective more exactly approximating the illness class with the least amount of computational work.

7. Conclusion

The suggested framework which relies on the attention GRU technique, was effective for classifying and identifying skin diseases with the least amount of computing work. The results show promise, including an accuracy of 97.3% when tested against different methods using real-time images from Kaggle. The model would become more reliable by adding information about present state finished weights optimisation. Additionally, it is contrasted several out-dated models like CNN, FTNN, and HARIS. shown in Results and Discussion section, suggested approach has demonstrated superior performance in categorization & analysing a growth trajectory according to textured-based data. But there are now a number of issues and will need to be fixed in further work. If the precision of the model is tested against a collection of photos taken in less-than-ideal lighting circumstances that are different from the ones used during testing, it is noticeably summary to slightly under 80%. In end, optional approach designed to support rather than replace the present approaches of illness diagnosis.

Reference

[1] H. W. Lim *et al.*, "The burden of skin disease in the United States," *J. Am. Acad. Dermatol.*, vol. 76, no. 5, pp. 958-972.e2, May 2017, doi: 10.1016/j.jaad.2016.12.043.

[2] G. Reynolds *et al.*, "Developmental cell programs are co-opted in inflammatory skin disease," *Science*, vol. 371, no. 6527, p. eaba6500, Jan. 2021, doi: 10.1126/science.aba6500.

[3] E. Pärna, A. Aluoja, and K. Kingo, "Quality of Life and Emotional State in Chronic Skin Disease," *Acta Derm. Venereol.*, vol. 95, no. 3, pp. 312–316, 2015, doi: 10.2340/00015555-1920.

[4] X. Sun, J. Yang, M. Sun, and K. Wang, "A Benchmark for Automatic Visual Classification of Clinical Skin Disease Images," in *Computer Vision – ECCV 2016*, B. Leibe, J. Matas, N. Sebe, and M. Welling, Eds., in Lecture Notes in Computer Science, vol. 9910. Cham: Springer International Publishing, 2016, pp. 206–222. doi: 10.1007/978-3-319-46466-4_13.

[5] B. Soutou and S. Aractingi, "Skin disease in pregnancy," *Best Pract. Res. Clin. Obstet. Gynaecol.*, vol. 29, no. 5, pp. 732–740, Jul. 2015, doi: 10.1016/j.bpobgyn.2015.03.005.

[6] J. Flannery *et al.*, "A novel strain of lumpy skin disease virus causes clinical disease in cattle in Hong Kong," *Transbound. Emerg. Dis.*, vol. 69, no. 4, Jul. 2022, doi: 10.1111/tbed.14304.

[7] B. Sanz-Bernardo *et al.*, "Quantifying and Modeling the Acquisition and Retention of Lumpy Skin Disease Virus by Hematophagus Insects Reveals Clinically but Not Subclinically Affected Cattle Are Promoters of Viral Transmission and Key Targets for Control of Disease Outbreaks," *J. Virol.*, vol. 95, no. 9, pp. e02239-20, Apr. 2021, doi: 10.1128/JVI.02239-20.

[8] D. Castillo, V. Lakshminarayanan, and M. J. Rodríguez-Álvarez, "MR Images, Brain Lesions, and Deep Learning," *Appl. Sci.*, vol. 11, no. 4, p. 1675, Feb. 2021, doi: 10.3390/app11041675.

[9] J. G. SivaSai, P. N. Srinivasu, M. N. Sindhuri, K. Rohitha, and S. Deepika, "An Automated Segmentation of Brain MR Image Through Fuzzy Recurrent Neural Network," in *Bio-inspired Neurocomputing*, A. K.

Bhoi, P. K. Mallick, C.-M. Liu, and V. E. Balas, Eds., in Studies in Computational Intelligence, vol. 903. Singapore: Springer Singapore, 2021, pp. 163–179. doi: 10.1007/978-981-15-5495-7_9.
[10] P. N. Srinivasu, J. G. SivaSai, M. F. Ijaz, A. K. Bhoi, W. Kim, and J. J. Kang, "Classification of Skin Disease Using Deep Learning Neural Networks with MobileNet V2 and LSTM," *Sensors*, vol. 21, no. 8, p. 2852, Apr. 2021, doi: 10.3390/s21082852.
[11] "Studies_on_Different_CNN_Algorithms_for_Face_Skin_Diseas.pdf."
[12] J. Kawahara, S. Daneshvar, G. Argenziano, and G. Hamarneh, "Seven-Point Checklist and Skin Lesion Classification Using Multitask Multimodal Neural Nets," *IEEE J. Biomed. Health Inform.*, vol. 23, no. 2, pp. 538–546, Mar. 2019, doi: 10.1109/JBHI.2018.2824327.
[13] A. Romero-Lopez, X. Giro-i-Nieto, J. Burdick, and O. Marques, "Skin Lesion Classification from Dermoscopic Images Using Deep Learning Techniques," in *Biomedical Engineering*, Innsbruck, Austria: ACTAPRESS, 2017. doi: 10.2316/P.2017.852-053.
[14] X. Li *et al.*, "Deep Learning Attention Mechanism in Medical Image Analysis: Basics and Beyonds," *Int. J. Netw. Dyn. Intell.*, Feb. 2023, doi: 10.53941/ijndi0201006.
[15] A. Esteva *et al.*, "Dermatologist-level classification of skin cancer with deep neural networks," *Nature*, vol. 542, no. 7639, pp. 115–118, Feb. 2017, doi: 10.1038/nature21056.
[16] N. Gessert *et al.*, "Skin Lesion Classification Using CNNs With Patch-Based Attention and Diagnosis-Guided Loss Weighting," *IEEE Trans. Biomed. Eng.*, vol. 67, no. 2, pp. 495–503, Feb. 2020, doi: 10.1109/TBME.2019.2915839.
[17] T. Li, Y. Zhang, and T. Wang, "SRPM–CNN: a combined model based on slide relative position matrix and CNN for time series classification," *Complex Intell. Syst.*, vol. 7, no. 3, pp. 1619–1631, Jun. 2021, doi: 10.1007/s40747-021-00296-y.
[18] F. An, X. Li, and X. Ma, "Medical Image Classification Algorithm Based on Visual Attention Mechanism-MCNN," *Oxid. Med. Cell. Longev.*, vol. 2021, pp. 1–12, Feb. 2021, doi: 10.1155/2021/6280690.
[19] L. Fu, B. Lu, B. Nie, Z. Peng, H. Liu, and X. Pi, "Hybrid Network with Attention Mechanism for Detection and Location of Myocardial Infarction Based on 12-Lead Electrocardiogram Signals," *Sensors*, vol. 20, no. 4, p. 1020, Feb. 2020, doi: 10.3390/s20041020.
[20] H. Wu, J. Pan, Z. Li, Z. Wen, and J. Qin, "Automated Skin Lesion Segmentation Via an Adaptive Dual Attention Module," *IEEE Trans. Med. Imaging*, vol. 40, no. 1, pp. 357–370, Jan. 2021, doi: 10.1109/TMI.2020.3027341.
[21] P. Pramanik, S. Mukhopadhyay, S. Mirjalili, and R. Sarkar, "Deep feature selection using local search embedded social ski-driver optimization algorithm for breast cancer detection in mammograms," *Neural Comput. Appl.*, vol. 35, no. 7, pp. 5479–5499, Mar. 2023, doi: 10.1007/s00521-022-07895-x.
[22] S. Alzahrani, B. Al-Bander, and W. Al-Nuaimy, "Attention Mechanism Guided Deep Regression Model for Acne Severity Grading," *Computers*, vol. 11, no. 3, p. 31, Feb. 2022, doi: 10.3390/computers11030031.
[23] S. Albahli, N. Nida, A. Irtaza, M. H. Yousaf, and M. T. Mahmood, "Melanoma Lesion Detection and Segmentation Using YOLOv4-DarkNet and Active Contour," *IEEE Access*, vol. 8, pp. 198403–198414, 2020, doi: 10.1109/ACCESS.2020.3035345.
[24] P. Yao *et al.*, "Single Model Deep Learning on Imbalanced Small Datasets for Skin Lesion Classification," *IEEE Trans. Med. Imaging*, vol. 41, no. 5, pp. 1242–1254, May 2022, doi: 10.1109/TMI.2021.3136682.
[25] P. N. Srinivasu, J. G. SivaSai, M. F. Ijaz, A. K. Bhoi, W. Kim, and J. J. Kang, "Classification of Skin Disease Using Deep Learning Neural Networks with MobileNet V2 and LSTM," *Sensors*, vol. 21, no. 8, p. 2852, Apr. 2021, doi: 10.3390/s21082852.
[26] Vellore Institute of Technology, Vellore, Tamilnadu, India, A. Victor, M. Ghalib, and Vellore Institute of Technology, Vellore, Tamilnadu, India, "Automatic Detection and Classification of Skin Cancer," *Int. J. Intell. Eng. Syst.*, vol. 10, no. 3, pp. 444–451, Jun. 2017, doi: 10.22266/ijies2017.0630.50.
[27] H. Niu, K. Xu, and C. Liu, "A decomposition-ensemble model with regrouping method and attention-based gated recurrent unit network for energy price prediction," *Energy*, vol. 231, p. 120941, Sep. 2021, doi: 10.1016/j.energy.2021.120941.
[28] L. Ma, J. Li, and Y. Zhao, "Population Forecast of China's Rural Community Based on CFANGBM and Improved Aquila Optimizer Algorithm," *Fractal Fract.*, vol. 5, no. 4, p. 190, Oct. 2021, doi: 10.3390/fractalfract5040190.
[29] P. Naga Srinivasu, T. Srinivasa Rao, and V. E. Balas, "A systematic approach for identification of tumor regions in the human brain through HARIS algorithm," in *Deep Learning Techniques for Biomedical and Health Informatics*, Elsevier, 2020, pp. 97–118. doi: 10.1016/B978-0-12-819061-6.00004-5.
[30] E. Cetinic, T. Lipic, and S. Grgic, "Fine-tuning Convolutional Neural Networks for fine art classification," *Expert Syst. Appl.*, vol. 114, pp. 107–118, Dec. 2018, doi: 10.1016/j.eswa.2018.07.026.

[31] J. Rathod, V. Waghmode, A. Sodha, and P. Bhavathankar, "Diagnosis of skin diseases using Convolutional Neural Networks," in *2018 Second International Conference on Electronics, Communication and Aerospace Technology (ICECA)*, Coimbatore: IEEE, Mar. 2018, pp. 1048–1051. doi: 10.1109/ICECA.2018.8474593.

[32] K. Simonyan and A. Zisserman, "Very Deep Convolutional Networks for Large-Scale Image Recognition," 2014, doi: 10.48550/ARXIV.1409.1556.

[33] A. G. Howard *et al.*, "MobileNets: Efficient Convolutional Neural Networks for Mobile Vision Applications," 2017, doi: 10.48550/ARXIV.1704.04861.

[34] C. A. Hartanto and A. Wibowo, "Development of Mobile Skin Cancer Detection using Faster R-CNN and MobileNet v2 Model," in *2020 7th International Conference on Information Technology, Computer, and Electrical Engineering (ICITACEE)*, Semarang, Indonesia: IEEE, Sep. 2020, pp. 58–63. doi: 10.1109/ICITACEE50144.2020.9239197.